



THE UNIVERSITY *of* EDINBURGH

## Edinburgh Research Explorer

### Hypomyelinating leukodystrophies

**Citation for published version:**

Pouwels, PJW, Vanderver, A, Bernard, G, Wolf, NI, Dreha-Kulczewski, SF, Deoni, SCL, Bertini, E, Kohlschütter, A, Richardson, W, Ffrench-Constant, C, Köhler, W, Rowitch, D & Barkovich, AJ 2014, 'Hypomyelinating leukodystrophies: Translational research progress and prospects', *Annals of Neurology*, vol. 76, no. 1, pp. 5-19. <https://doi.org/10.1002/ana.24194>

**Digital Object Identifier (DOI):**

[10.1002/ana.24194](https://doi.org/10.1002/ana.24194)

**Link:**

[Link to publication record in Edinburgh Research Explorer](#)

**Document Version:**

Publisher's PDF, also known as Version of record

**Published In:**

Annals of Neurology

**Publisher Rights Statement:**

Available under Open Access

**General rights**

Copyright for the publications made accessible via the Edinburgh Research Explorer is retained by the author(s) and / or other copyright owners and it is a condition of accessing these publications that users recognise and abide by the legal requirements associated with these rights.

**Take down policy**

The University of Edinburgh has made every reasonable effort to ensure that Edinburgh Research Explorer content complies with UK legislation. If you believe that the public display of this file breaches copyright please contact [openaccess@ed.ac.uk](mailto:openaccess@ed.ac.uk) providing details, and we will remove access to the work immediately and investigate your claim.



# Hypomyelinating Leukodystrophies: Translational Research Progress and Prospects

Petra J. W. Pouwels, PhD,<sup>1</sup> Adeline Vanderver, MD,<sup>2</sup>  
Genevieve Bernard, MD, MSc, FRCPC,<sup>3</sup> Nicole I. Wolf, MD, PhD,<sup>4</sup>  
Steffi F. Dreha-Kulczewski, MD,<sup>5</sup> Sean C. L. Deoni, PhD,<sup>6</sup> Enrico Bertini, MD, PhD,<sup>7</sup>  
Alfried Kohlschütter, MD,<sup>8</sup> William Richardson, FMedSci, FRS,<sup>9</sup>  
Charles French-Constant, PhD,<sup>9</sup> Wolfgang Köhler, MD,<sup>10</sup> David Rowitch, MD, PhD,<sup>11</sup>  
and A. James Barkovich, MD<sup>12,13</sup>

Hypomyelinating leukodystrophies represent a genetically heterogeneous but clinically overlapping group of heritable disorders. Current management approaches in the care of the patient with a hypomyelinating leukodystrophy include use of serial magnetic resonance imaging (MRI) to establish and monitor hypomyelination, molecular diagnostics to determine a specific etiology, and equally importantly, careful attention to neurologic complications over time. Emerging research in oligodendrocyte biology and neuroradiology with bedside applications may result in the possibility of clinical trials in the near term, yet there are significant gaps in knowledge in disease classification, characterization, and outcome measures in this group of disorders. Here we review the biological background of myelination, the clinical and genetic variability in hypomyelinating leukodystrophies, and the insights that can be obtained from current MRI techniques. In addition, we discuss ongoing research approaches to define potential outcome markers for future clinical trials.

ANN NEUROL 2014;76:5–19

The concept of hypomyelinating disorders was originated by Schiffmann, van der Knaap, and colleagues.<sup>1–3</sup> Among the inherited white matter (WM) disorders, hypomyelinating leukodystrophies (HLDs) are notable for abnormalities in myelin development rather than destruction. This class of disorders is distinguished by their characteristic appearance on magnetic resonance imaging (MRI), namely, lessening or absence of the T<sub>2</sub> hypointensity that typically signifies the presence of mye-

lin, often without the significant lessening of T<sub>1</sub> hyperintensity seen in the other, nonhypomyelinating leukodystrophies. Other MRI features help to narrow the differential diagnosis and focus genetic and metabolic testing.<sup>3</sup>

We are entering a phase of clinical research for HLDs where identification of outcome measures of potential treatment benefit is crucial. In ultrarare diseases, clinical features, and natural history are often

View this article online at [wileyonlinelibrary.com](http://wileyonlinelibrary.com). DOI: 10.1002/ana.24194

Received Mar 4, 2014, and in revised form Jun 5, 2014. Accepted for publication Jun 5, 2014.

Address correspondence to Dr Barkovich, 505 Parnassus Ave, Long, San Francisco, CA 94143-0734. E-mail: [James.Barkovich@ucsf.edu](mailto:James.Barkovich@ucsf.edu)

From the <sup>1</sup>Department of Physics and Medical Technology, VU University Medical Center and Neuroscience Campus Amsterdam, Amsterdam, the Netherlands; <sup>2</sup>Department of Neurology, Children's National Medical Center, Washington, DC; <sup>3</sup>Departments of Pediatrics, Neurology, and Neurosurgery, Montreal Children's Hospital, McGill University Health Center, Montreal, Quebec, Canada; <sup>4</sup>Department of Child Neurology, VU University Medical Center and Neuroscience Campus Amsterdam, Amsterdam, the Netherlands; <sup>5</sup>Department of Pediatrics and Pediatric Neurology, University Medical Center, Göttingen, Germany; <sup>6</sup>Advanced Baby Imaging Laboratory, Brown University School of Engineering, Providence, RI; <sup>7</sup>Unit of Neuromuscular and Neurodegenerative Disorders, Laboratory of Molecular Medicine, Bambino Gesù Children's Research Hospital, Rome, Italy; <sup>8</sup>Department of Pediatrics, University Medical Center Hamburg-Eppendorf, Hamburg, Germany; <sup>9</sup>Wolfson Institute for Biomedical Research, University College London, London, United Kingdom; <sup>10</sup>MRC Centre for Regenerative Medicine, University of Edinburgh, Edinburgh, UK; <sup>11</sup>Department of Neurology, Hubertusburg Specialized Hospital, Wermsdorf, Germany; <sup>12</sup>Departments of Pediatrics and Neurological Surgery, University of California, San Francisco, San Francisco, CA; and <sup>13</sup>Department of Radiology and Biomedical Imaging and Department of Neurology, University of California, San Francisco, San Francisco, CA.

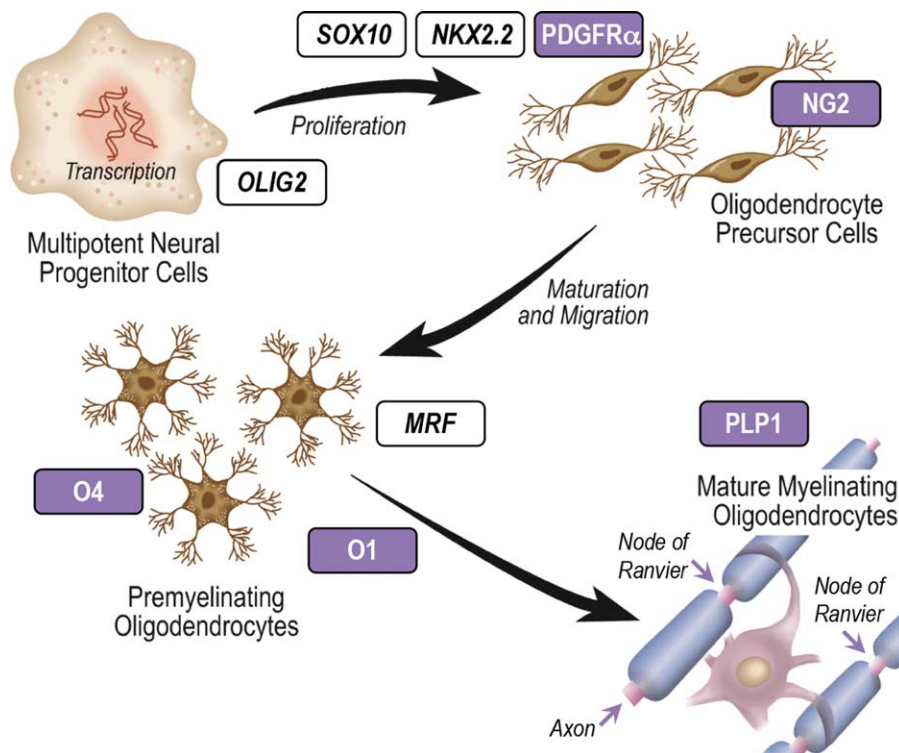


**FIGURE 1:** Overview of oligodendrocyte lineage development. Oligodendrocyte development commences in the midgestation mammalian embryo. Multipotent neural progenitor cells competent to produce oligodendrocytes express the transcription factor OLIG2, and cell intrinsic and environmental interactions with other transcription factors (eg, SOX10, NKX2.2) lead to specification of oligodendrocyte precursor cells (OPCs) marked by expression of platelet-derived growth factor receptor- $\alpha$  (PDGFR $\alpha$ ) and neuron-glia antigen 2 (NG2). Such OPCs proliferate after specification, migrate throughout the central nervous system parenchyma, and differentiate under control of myelin regulatory factor (MRF) and other intrinsic programs. In white matter, premyelinating oligodendrocytes engage with axons, and it is thought that physical and activity-dependent cues trigger myelin wrapping, marked initially by transition from O4<sup>+</sup> to O1<sup>+</sup> stages, and eventually expression of proteolipid protein 1 (PLP1) and other mature markers. One oligodendrocyte can provide hundreds of myelin segments to adjacent axons. Myelination enables formation of nodes of Ranvier, which cluster sodium channels for saltatory conduction. Myelination is also thought to stabilize axonal membranes, which results in physical properties detectable by magnetic resonance imaging. Transcription factors are indicated by unfilled boxes and cellular markers by violet/filled boxes.

poorly known; therefore, clinical/neurological parameters alone are insufficient as endpoints for clinical efficacy studies. In this case, another possible acceptable clinical trial design includes the use of biomarkers as surrogate endpoints. The adoption of criteria for biomarkers of efficacy is an important feasibility step for the planning and execution of clinical studies because it provides an objective endpoint at a defined period of time after an intervention has been initiated. Proposing a standard measure of myelination based upon magnetic resonance (MR) metrics as a reliable biomarker could therefore greatly encourage clinical research.

With these challenges in mind, we organized a multidisciplinary group to address clinical and future research priorities for HLDs. The group makes consensus recommendations for MRI and neurological assessments in clinical care, endpoints for clinical research, and potential methods to detect myelin in the human brain with greater specificity and sensitivity.

### Biological Basis of Myelination and HLDs

Oligodendrocytes are the myelinating cells of the central nervous system (CNS; Fig 1). Myelin enables rapid transmission of action potentials through saltatory conduction,<sup>4,5</sup> provides trophic support and protection for axons,<sup>6–8</sup> and allows for packing of greater axon densities during the evolution of brain complexity.<sup>9</sup> Almost half of the human brain is comprised of tracts of myelinated axons in WM, and it is therefore not surprising that leukodystrophies, caused by deficient deposition or destruction of myelin, have significant functional effects.

Myelination is an energy-expensive process, as developing oligodendrocyte precursor cells (OPCs) undergo as much as a 6,500-fold increase in membrane surface area as they differentiate into oligodendrocytes that provide up to ~100 myelin segments on multiple axons through extension of protoplasmic processes.<sup>10,11</sup> Mature oligodendrocytes also provide ongoing trophic support to axons, in part through functions of the

monocarboxylate transporter 1.<sup>12,13</sup> Finally, initiation of myelination and myelin maintenance is regulated by the availability of glycolytic and lipid substrates such as purines, glucose, and lactate.<sup>6,14</sup> OPCs are widespread in the normal adult CNS, where they contribute to myelin repair (eg, in multiple sclerosis<sup>15</sup>) and turnover of myelin within normal WM.<sup>16</sup>

The focus of this review will be the HLDs. As shown in Figure 1, early oligodendrocyte development comes under control by specific transcription factors that promote glial subtype specification of OPCs. Transcription factors Olig2, Sox10, and Nkx2.2 are essential for early stages of OPC development, whereas other transcriptional proteins, including myelin regulatory factor (MyRF), as well as chromatin remodeling and signaling pathways such as integrin and PI3 kinase, coordinate to promote later stages of oligodendrocyte differentiation

and myelin remodeling.<sup>17,18</sup> No HLD-causing mutations have been identified in these pathways, perhaps because they are essential in many cell types. The sheath then formed is enriched in myelin-specific lipids and proteins including proteolipid protein 1 (PLP1). Mutations in *PLP1* are known to be causative of Pelizaeus–Merzbacher disease (PMD), a classic example of an HLD. Different types of mutations in *PLP1* may have different impacts on the oligodendrocyte lineage. The most common alteration is duplication of the entire gene, suggesting that gene dosage is essential. Severe missense mutations in *PLP1* trigger the unfolded protein response and cell death of OPCs, preventing myelination, leading to the severe congenital form of the disease.<sup>19</sup> Milder missense mutations and null mutations are associated with milder forms. Although OPCs likely respond to the loss of myelin in HLDs, their intrinsic mutation likely renders them ineffective in repair.

## Diagnosis and Management of HLDs

HLDs are characterized by a paucity of myelin development based on histochemistry and MRI criteria. MRI typically shows variable signal (ie, hyper-, hypo-, or iso-intense) on T<sub>1</sub>-weighted imaging and mild hyperintensity on T<sub>2</sub>-weighted imaging of the WM compared to gray matter (GM) signal (Fig 2A–F).<sup>2</sup> This is distinct from other leukodystrophies, in which more hypointense

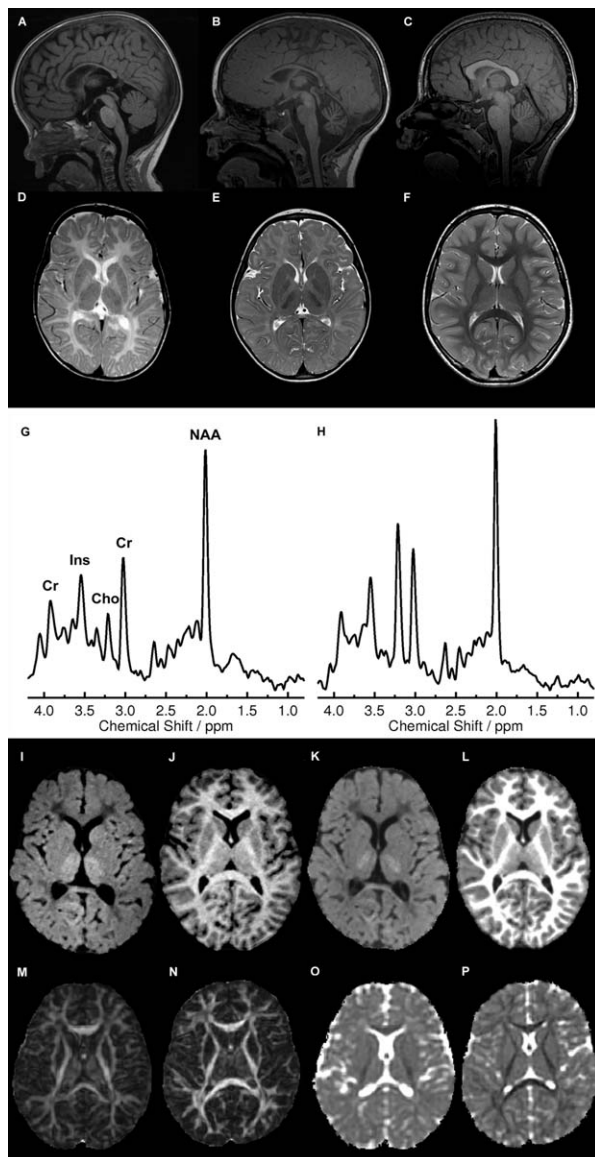


**FIGURE 2: Magnetic resonance imaging (MRI) of hypomyelinating leukodystrophy patients in comparison to subjects with normal MRI.** (A–C) Sagittal T<sub>1</sub>-weighted images show hypointense signal of corpus callosum in (A) a 4-year-old Pelizaeus–Merzbacher disease (PMD) patient and (B) additional cerebellar atrophy in a 2-year-old hypomyelination, hypodontia, and hypogonadotropic hypogonadism (4H) patient, in comparison to (C) a 5-year-old control subject. (D–F) Axial T<sub>2</sub>-weighted images show homogeneous T<sub>2</sub> hyperintensity of white matter in (D) a 4-year-old PMD patient and similar white matter hyperintensity in addition to hypointensity of the globi pallidi and lateral thalami in (E) a 2-year-old 4H patient in comparison to (F) a 5-year-old control subject. (G, H) Magnetic resonance spectrum of white matter in (G) a 4H patient shows reduced choline (Cho) in comparison to (H) a 5-year-old control subject. (I, J) Magnetization transfer (MT) ratio maps and (K, L) MT saturation maps show severe global reduction of MT values (manifested as decreased hyperintensity) in (I, K) a 6-year-old 4H patient compared to (J, L) a 6-year-old control subject. (M, N) Fractional anisotropy (FA) maps and (O, P) radial diffusivity (RD) maps show a reduction of FA (manifested as decreased white matter hyperintensity in M compared with N) and an increase of RD (manifested as less white matter hypointensity in O compared with P) in a 4-year-old 4H patient (M, O) in comparison to a 7-year-old control subject (N, P). The images of each pair I–J, K–L, M–N, and O–P are shown at the same intensity scale. Cr = creatine; Ins = inositol; NAA = N-acetylaspartate.

**TABLE 1. Hypomyelinating Leukodystrophies, Their Inheritance, and Their Respective Genetic Cause, When Known**

Hypomyelinating Disorder	OMIM Number	Abbreviation	Inheritance	Gene
18q- syndrome	601808		Sporadic	<i>18q-</i>
Cockayne syndrome	216400		AR	<i>ERCC6, ERCC8</i>
Hypomyelination with atrophy of the basal ganglia and cerebellum	612438	H-ABC	Sporadic	<i>TUBB4A</i>
Hypomyelination with congenital cataracts	610532	HCC	AR	<i>FAM126A</i>
Hypomyelination of early myelinated structures		HEMS	X-linked	<i>unknown</i>
Hypomyelination with brainstem and spinal cord involvement and leg spasticity	615281	HBSL	AR	<i>DARS</i>
Free sialic acid storage disease	604369		AR	<i>SLC17A5</i>
Fucosidosis	230000		AR	<i>FUCA1</i>
Pelizaeus–Merzbacher disease	312920	PMD	X-linked	<i>PLP1</i>
Pelizaeus–Merzbacher–like disease	608804	PMLD	AR	<i>GJC2</i>
Pol III-related leukodystrophies/4H	607694, 614381	4H	AR	<i>POLR3A, POLR3B</i>
Oculodentodigital dysplasia	164200	ODDD	AD, sporadic	<i>GJA1</i>
<i>RARS</i> -associated hypomyelination, <i>SOX10</i> -associated disorders	609136		AR, AD, sporadic	<i>RARS, SOX10</i>
Trichothiodystrophy with hypersensitivity to sunlight	601675		AR	<i>ERCC2, ERCC3, GTF2H5, MPLKIP</i>

4H = hypomyelination, hypodontia, and hypogonadotropic hypogonadism; AD = autosomal dominant; AR = autosomal recessive; OMIM = Online Mendelian Inheritance in Man database.

T<sub>1</sub>-weighted and more severely hyperintense T<sub>2</sub>-weighted WM imaging signals are seen, usually in a more geographic or localized distribution.

It is also important to differentiate HLDs from neuronal diseases with secondary hypomyelination, which carry an independent differential diagnosis, such as *AGC1*-,<sup>20,21</sup> *HSPD1*-,<sup>22</sup> and *AIMP1*-related disorders.<sup>23,24</sup> Neuronal diseases with secondary hypomyelination have prominent GM symptoms, such as early onset epilepsy and severe intellectual disability. They commonly present with microcephaly and/or early and severe cerebral atrophy. It is also important to differentiate HLDs from delayed myelination. When a lack of myelin deposition is noticed on an MRI in a child younger than 2 years, a second MRI should be performed at least 6 months later to assess for significantly improved myelination, diagnostic of delayed myelination (in distinction, increase in myelination is not observed in HLDs).

HLDs are genetically and clinically diverse (Table 1), but have commonalities as a group. Most HLD patients present in the neonatal or infantile period with

axial hypotonia, which evolves to spastic quadriparesis, and have or will develop nystagmus. Patients with PMD, Pelizaeus–Merzbacher–like disease caused by mutations in *GJC2*,<sup>25</sup> and *SOX10*-related disorders<sup>26</sup> have early onset of congenital nystagmus, whereas patients with hypomyelination, hypodontia, and hypogonadotropic hypogonadism (4H),<sup>27,28</sup> oculodentodigital dysplasia, and 18q-syndrome develop nystagmus later in the course of their disease or never. Cerebellar signs are often present and can be the predominant clinical manifestation, such as in 4H, a RNA polymerase III–related leukodystrophy. Extrapyramidal signs are not uncommon, especially dystonia, but typically occur later in the disease course, with the exception of hypomyelination with atrophy of the basal ganglia and cerebellum (H-ABC), where dystonia is often seen early in the disease. Cognitive function is relatively preserved in most patients but typically declines slowly or relatively late in the disease course. Another possible neurological manifestation of HLDs is the presence of a peripheral neuropathy, which can be seen inconsistently with *PLP*-null syndrome (one of the



**TABLE 2. MRI Characteristics and the Diagnoses They Suggest**

MRI Characteristic	Suggests
Diffuse and homogeneous hypomyelination	PMD
Diffuse and homogeneous hypomyelination with hypomyelination of the brainstem, especially the pons	PMLD
Hypomyelination with areas of increased T <sub>2</sub> signal and decreased T <sub>1</sub> signal	HCC, 18q- syndrome, HBSL
Relative T <sub>2</sub> hypointensity of the dentate nuclei, optic radiation, globi pallidi, anterolateral nuclei of the thalami, corticospinal tract at the level of the PLIC	Pol III/4H
Hypomyelination of early myelinating structures	HEMS
Calcifications	Cockayne syndrome, AGS <sup>a</sup>
Thin corpus callosum	Pol III/4H, fucosidosis, Cockayne syndrome, sialic acid storage disease
Cerebellar atrophy	Pol III/4H, sialic acid storage disease, H-ABC, ODDD, Cockayne syndrome, fucosidosis, 18q- syndrome (hypoplasia)
Basal ganglia abnormalities	Atrophy (especially putamen), H-ABC; hyper T <sub>1</sub> and hypo T <sub>2</sub> of GP; fucosidosis; hypo T <sub>2</sub> of GP; Pol III/4H, ODDD
Prominent cerebral atrophy	Infantile sialic acid storage disease, AGS <sup>a</sup>

4H = hypomyelination, hypodontia, and hypogonadotropic hypogonadism; AGS = Aicardi–Goutières syndrome; GP = globus pallidus; H-ABC = hypomyelination with atrophy of the basal ganglia and the cerebellum; HBSL = hypomyelination with brainstem and spinal cord involvement and leg spasticity; HCC = hypomyelination with congenital cataracts; HEMS = hypomyelination of early myelinating structures; hyper = hyperintensity; hypo = hypointensity; MRI = magnetic resonance imaging; ODD- D = oculodentodigital dysplasia; PLIC = posterior limb of the internal capsule; PMD = Pelizaeus–Merzbacher disease; PMLD = PMD-like; Pol III = Pol III-related leukodystrophies.

<sup>a</sup>AGS may present with a hypomyelinating pattern on MRI.

milder PMD forms), Cockayne syndrome, *SOX10*-related disorders, and hypomyelination with congenital cataracts (HCC). A full description of these conditions and the reasons they are included within the HLDs is beyond the scope of this review and described elsewhere.<sup>29</sup>

Some HLDs can present with an adult onset hereditary spastic paraparesis phenotype. In addition to progressive spastic paraplegia, dysarthria, dysphagia, and later cognitive decline are frequent in adulthood. The late onset HLD phenotypes have much milder MRI WM abnormalities. In 4H, some affected patients present in late adolescence or early adulthood with hypomyelination on MRI that is not well correlated with the disease severity. A late presentation is often associated with milder clinical symptoms and slower deterioration. A spectrum with more severe infantile onset cases on one end and milder adolescent or adult onset variants at the other extreme will probably be part of most if not all HLDs.

In the diagnosis of a HLD, MRI pattern recognition is very useful (Table 2),<sup>3</sup> but non-neurological

features, when present, can help the clinician in suspecting one disorder versus another (Table 3). For example, hypodontia and delayed puberty point to 4H, whereas the presence of cataracts suggests HCC. Overall, it is important to note that these systemic manifestations are inconstant and may not be present in all affected individuals.

Molecular diagnosis has become the mainstay in diagnosis of hypomyelinating conditions, and a targeted number of genes specific to hypomyelination should be tested. A definitive molecular diagnosis will aid the clinician with management, prognosis, and genetic counseling.

Management of patients with HLDs will largely depend on the specific diagnosis and individual severity of the disease. Typical complications in patients with the classic form of PMD include severe spasticity necessitating oral or intrathecal treatment with baclofen, chemodenervation, or selective dorsal rhizotomy. Dystonia is seen more frequently in certain HLDs such as H-ABC and

**TABLE 3. Useful Non-Neurological Clinical Features to Orient the Diagnosis in Hypomyelinating Leukodystrophies**

Clinical Characteristics	Suggests
Dysmorphic signs	18q- syndrome
Facial coarsening	Sialic acid storage disease, fucosidosis
Cataracts	HCC, Cockayne syndrome, Pol III/4H (rarely)
Myopia, typically progressive and severe	Pol III/4H
Hearing loss	Cockayne syndrome, <i>SOX-10</i>
Dental abnormalities	Pol III/4H <sup>a</sup> ; Cockayne syndrome, propensity to cavities; ODDD, enamel hypoplasia
Skin abnormalities	Cockayne syndrome, hypersensitivity to sunlight; fucosidosis, angiokeratoma corporis diffusum
Hand and feet abnormalities	ODDD
Cardiac abnormalities	18q- syndrome; fucosidosis, cardiomegaly
Hepatosplenomegaly	Sialic acid storage disease, fucosidosis
Endocrine abnormalities	18q- syndrome, Pol III/4H (delayed or absent puberty)

<sup>a</sup>The dental abnormalities encountered in Pol III–related leukodystrophies are not universal and are highly variable: oligodontia, hypodontia, delayed teeth eruption, abnormal sequence of teeth eruption, and abnormal color or shape of sometimes 1 but typically several teeth.  
 4H = hypomyelination, hypodontia, and hypogonadotropic hypogonadism; HCC = hypomyelination with congenital cataracts; ODDD = oculodentodigital dysplasia; Pol III = Pol III–related leukodystrophies.

4H, and should be managed with appropriate pharmacotherapy. Scoliosis and hip dislocations are frequent complications, and should be carefully prevented and treated in a timely manner. Swallowing difficulties are present early in severe forms, and in milder forms develop over time. Epilepsy is an infrequent complication of HLDs. If present, appropriate treatment with antiepileptic drugs should be initiated. Specific complications of certain entities among the HLDs include endocrine abnormalities (hypogonadotropic hypogonadism and, less frequently, growth hormone deficiency) in 4H. Endocrine monitoring should be done regularly; treatment decisions should be made on an individual basis. Management of the dental anomalies in 4H includes prosthetic treatment and early detection of cavities.

### Myelin Assessment by MRI

In addition to conventional T<sub>1</sub>- and T<sub>2</sub>-weighted imaging, several advanced MRI techniques might be more appropriate to clinically detect myelin in the human brain. In the following sections, we discuss proton magnetic resonance spectroscopy (MRS), quantitative T<sub>1</sub> and T<sub>2</sub>, magnetization transfer imaging (MTI), and diffusion tensor imaging (DTI).

### Myelin Assessment by Proton MRS

Proton MRS allows separation of protons in different chemical environments based upon the effects of surrounding electron clouds upon the net strength of the magnetic field felt by the proton (chemical shift) and the influences of neighboring nuclei (spin–spin coupling). Used for decades in analytical chemistry, it has been applied to human diseases as a part of the MRI examination. Recently, MRS has been investigated as a tool in the assessment of metabolic disorders and specifically HLDs.<sup>30–32</sup> However, the spectrum of myelin itself is quite complex, essentially composed of overlapping spectra of the many functional groups that are part of the proteins and complex molecules that are components of myelin.<sup>33</sup> The peaks from most of the protons within these functional groups are split (into doublets, triplets, quadruplets, and more) by adjacent protons and/or have T<sub>2</sub> relaxation times too short to be apparent on in vivo proton spectra.<sup>34</sup> Therefore, the use of in vivo proton MRS in patients with disorders of myelin formation is mainly limited to assessment of the major peaks seen in the human brain: choline, creatine, myo-inositol, glutamate, glutamine, and N-acetylaspartate (NAA; see Fig 2G, H). None of these peaks has been shown to directly reflect the presence or quantity of myelin in the

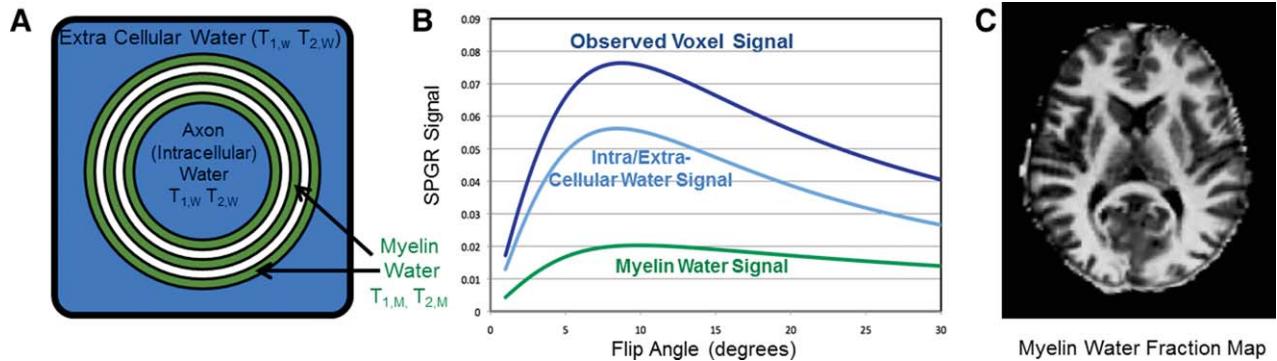


**FIGURE 3:** Background of myelin water fraction determination. (A) Because of more interactions with surrounding molecules and electrical/magnetic variations, myelin water has shorter relaxation times ( $T_{1,m}$  and  $T_{2,m}$ ) than intra-/extracellular water ( $T_{1,w}$  and  $T_{2,w}$ ). (B) The signal intensity per voxel is a combination of myelin water and intra-/extracellular water, as shown here for  $T_1$ -weighted spoiled gradient recalled (SPGR) as a function of flip angle. (C) Additional  $T_1/T_2$ -weighted sequences allow for the estimation of a myelin water fraction map.<sup>62</sup>

developing brain, although combinations of peak heights can be used to roughly monitor normal brain development.<sup>35–37</sup>

Some authors have studied proton MRS in HLDs and compared them with other leukodystrophies.<sup>38</sup> They found high creatine and myo-inositol levels and low choline levels compared to controls.<sup>38</sup> Takanashi et al have studied the use of proton MRS in 2 mouse models of HLDs, the *msd* mouse (a model of congenital PMD)<sup>31</sup> and the *shiverer* (*Shi*) mouse (deficient for myelin basic protein),<sup>39</sup> and found very different proton MRS patterns. NAA, which is normally metabolized to acetate and aspartate in oligodendrocytes,<sup>40</sup> is elevated in the classic form of PMD.<sup>30,32</sup> The most likely reason for this is that the PLP1 proteins in PMD patients are abnormally folded and accumulated in the endoplasmic reticulum, resulting in the activation of an unfolded protein response that finally leads to oligodendrocyte apoptotic death before normal myelination occurs, leading to higher NAA levels.<sup>41</sup> In contrast, NAA is low in *Shi* mice, presumably because the number of cortical neurons is decreased<sup>39</sup> for reasons that are not currently understood. Choline may be reduced in HLDs, as cultured oligodendrocytes have a higher concentration of choline than neurons, astrocytes, or oligodendrocyte precursors.<sup>42</sup> However, at this time, it does not seem that MRS will be useful by itself to quantify myelination.

### Myelin Assessment by Quantitative $T_1$ and $T_2$

Much of the exquisite soft tissue contrast we have come to expect from MRI arises from differences in the intrinsic  $T_1$  and  $T_2$  relaxation properties. In their most basic description, both  $T_1$  and  $T_2$  relaxation processes result from molecular motion and interactions, which are influenced by the biophysical structure and biochemical envi-

ronment.<sup>43</sup> In particular, characteristics such as density (ie, water content/mobility); macromolecule, protein, and lipid composition; and paramagnetic atom (eg, iron) concentrations alter the local tissue environment, and consequently affect tissue  $T_1$  and  $T_2$ . In WM, for example, the phospholipid-rich myelin sheath and associated proteins, cholesterol, iron-containing oligodendrocytes and glial cells, and reduced free water content all result in decreased  $T_1$  and  $T_2$  relative to GM.<sup>44</sup> These relaxation time differences are readily apparent in the GM/WM contrast in conventional  $T_1$ - and  $T_2$ -weighted images of adult brain, and onset or alteration of this contrast has been used as a qualitative measure of myelin changes. For example, the emergence of GM/WM contrast in the developing brain, associated with drastic reductions in the  $T_1$  and  $T_2$  relaxation times, broadly parallels the histological timeline of myelination.<sup>35</sup> Similarly, a change of contrast driven by prolonged  $T_1$  and  $T_2$  in WM disorders, such as multiple sclerosis, can primarily reflect focal myelin loss.<sup>45</sup>

Relaxation properties are extremely sensitive to local microstructural and biochemical changes in WM, but they are nonspecific and can reflect developing myelination, differing concentrations of iron (ferritin),<sup>46</sup> water content changes associated with fiber density and diameter, or pathological processes such as edema and inflammation.<sup>47</sup> In an effort to improve myelin sensitivity and specificity, a multiple-component approach has been proposed.<sup>48–50</sup> Here, the  $T_1$  and/or  $T_2$  signal curves observed within an imaging voxel are assumed to be a composite mixture from multiple distinct microanatomical tissue environments that, through their unique microstructure and biochemistry, have differing  $T_1$  and  $T_2$  characteristics and thus distinct MRI signal signatures (Fig 3A, B). The aim of multiple component relaxation analysis is to decompose and quantify these individual



signatures, allowing more direct assessment of myelin content. Conventionally, this has been accomplished through the acquisition of multiple<sup>32–48</sup> spin-echo  $T_2$  decay data spanning a wide range of echo times (up to 320 milliseconds).<sup>51</sup> Assuming a slow exchange regime with respect to  $T_2$ ,<sup>52</sup> a non-negative least squares approach is used to fit a semicontinuous log  $T_2$  distribution to the sampled decay data.<sup>51</sup> Results of this fitting have consistently revealed a bi- or trimodal  $T_2$  profile, with a short  $T_2$  peak ( $T_2 < 30$  milliseconds), moderate  $T_2$  peak ( $60 < T_2 < 150$  milliseconds), and a long  $T_2$  peak ( $T_2 > 2$  seconds).<sup>52</sup> Through imaging–histology comparisons<sup>53,54</sup> and in vivo studies of demyelinating disorders,<sup>55</sup> these peaks have been ascribed to 3 layers: water trapped between the lipid myelin bilayers; the less restricted intra- and extracellular water; and cerebrospinal fluid, respectively.<sup>51,52</sup> The volume ratio of the short  $T_2$  peak to the total area under the  $T_2$  distribution, termed the *myelin water fraction* (MWF), has strong correlation with histological assessments of myelin content,<sup>51,52</sup> irrespective of inflammation or changes in water content.<sup>56</sup> Recently, similar multicomponent  $T_1$  relaxation has been demonstrated at ultrahigh field strengths.<sup>57</sup> Thus, MWF has the potential to be a better quantitative marker of myelin than measures derived from MTI or DTI.<sup>58,59</sup> However, MWF has not yet gained entrance into routine clinical MRI because of limited spatial coverage, time requirements, and frequent technical difficulties that result in stimulated echo artifacts.

Due to the lengthy acquisition times required, recent work has centered on the development of 3-dimensional multicomponent relaxation approaches, such as rapid spiral imaging,<sup>60</sup> or alternative non-spin echo based imaging methodologies (ie, GRASE<sup>61</sup> or mcDESPOt<sup>62</sup>). These newer methods have the potential to overcome some of the difficulties in integrating MWF into standard clinical protocols (see Fig 3C), but need further validation.<sup>63</sup> They have already provided preliminary new insight into brain development and myelination,<sup>64</sup> as well as myelin changes that reflect disease course and severity in other WM disorders.<sup>65,66</sup>

### Myelin Assessment by MTI

MTI targets magnetization exchange between immobile macromolecular protons (bound pool), such as those bound in proteins and lipid bilayers of myelin, and free water protons (free pool). Magnetization transfer (MT) is evoked by selectively saturating the bound pool with an off-resonance radiofrequency pulse. This saturation is then transferred to the free pool and observed as an attenuation of the MR signal.<sup>67</sup> In WM the MT effect is

overproportionately determined by MWF,<sup>68</sup> suggesting that MT characteristics mainly relate to myelin.

Quantitative MT methods adopt complex modeling of the 2 pools, allowing mapping of multiple parameters with the bound pool fraction  $f$  being most relevant.<sup>69,70</sup> The bound pool is about 2 to 3× larger in WM (11%) than in GM (4%), small in blood (2%), and absent in cerebrospinal fluid.<sup>71</sup> In demyelination, strong correlations of  $f$  and magnetization transfer ratio (MTR) with histologically quantified myelin density have been detected in animal models<sup>72,73</sup> and in human postmortem multiple sclerosis studies.<sup>74,75</sup> However, bovine brain imaging and imaging–histology correlations have suggested that nonmyelin WM, containing macromolecules such as axonal membranes and glial cells, also modulate MT measures.<sup>75–77</sup> Moreover, general WM pathological changes in demyelinating diseases have been shown to influence and complicate MT measures of myelin.<sup>74,76,78</sup>

The utility of quantitative MT (qMT) parameters has benefited greatly from studies in hypomyelinating conditions such as those in *shaking* (*Sh*) pups, a canine model with a *PLP* gene mutation,<sup>79</sup> with  $f$  being most discriminative. Because axons are preserved in *Sh* pups, the results indicate a high correlation to normal myelination. Similar results have been obtained with qMT in hypomyelinating *Shi* mice.<sup>80,81</sup>

Not surprisingly, MTR has been found significantly decreased in childhood HLDs.<sup>38</sup> MT saturation maps in various HLDs in children revealed an overall decrease with distinct spatial distributions of higher MT saturation values, reflecting lack of myelin, and characteristic regions containing more myelin in accordance with histopathological findings (see Fig 2I–L).<sup>82</sup> The sensitivity to changes in myelination has rendered MT saturation a suitable parameter to monitor treatment effects, as demonstrated in cerebral folate transporter  $\alpha$  deficiency with hypomyelination. In preliminary studies, folinic acid treatment may improve/normalize MT saturation values (Dreha-Kulaczewski, unpublished observations).

### Myelin Assessment by DTI

DTI can be used to assess the magnitude and direction of water motion in a volume of tissue. If small volumes are imaged at high resolution, this technique gives insight into the microstructure of WM. Parallel myelinated axons give rise to a high fractional anisotropy (FA), indicating the direction of overall motion of water molecules in the sampled voxel. In WM, this direction is determined by the largest eigenvalue of the diffusion tensor, representing diffusivity parallel to the axons (axial diffusivity [AD]), and by the 2 lower eigenvalues, representing diffusivity perpendicular to the axons (radial diffusivity

[RD]).<sup>83</sup> RD has been interpreted as an indicator of myelin density, based on increased values in mouse models of hypomyelination, the *Shi* mouse,<sup>84</sup> the transgenic *hcv1-tk* mouse,<sup>85</sup> and the fixed brains of Plp1-transgenic mice.<sup>86</sup> AD has been interpreted as a measure of axonal integrity; it is normal in *Shi* mice with relatively intact axons, and decreased in *hcv1-tk* mice with reduced axonal caliber.<sup>84,85</sup> The increased RD in poorly myelinated WM has been confirmed in the *Sh* pup; of all investigated DTI parameters, the relative increase of RD was most prominent, whereas the increase of AD was much smaller, in accordance with paucity of myelin being the most apparent histopathological observation.<sup>87</sup> However, the actual quantification of myelin by means of these parameters has not yet been demonstrated.

It should be noted that the tensor model, although widely used, is limited by the assumption of a Gaussian distribution of water diffusion, and DTI parameters are sensitive to partial volume averaging, because the size of the voxels being assessed is much larger than that of the crossing fiber tracts.<sup>88</sup> To overcome these limitations, high b-value diffusion imaging was additionally applied in the abovementioned *Shi* pup study.<sup>87</sup> Results showed that the zero-displacement probability  $P_0$ , which is obtained from high b-value diffusion imaging and which describes the degree of water restriction in tissue, was similarly sensitive to the paucity of myelin as the DTI parameter RD, which is more widely available on clinical scanners.

Human DTI studies comparing FA, AD, and RD parameters indicate RD to be the most sensitive in distinguishing HLD patients from controls (see Fig 2M–P). A case study of a family with a unique mutation of PMD has described increases in the lowest eigenvalues,<sup>89</sup> and a preliminary study in a larger group of patients with several HLDs also identified RD as the most relevant DTI parameter (Steenweg et al, unpublished).

Although DTI parameters are indicative of myelin content, they are sensitive to changes in myelination, and thus may serve to detect treatment effects. With the *hsv-tk1* mouse model, which has a phenotype with a transient, reversible hypomyelination,<sup>85</sup> strongly elevated RD was observed at 2 weeks of age, which normalized in the following weeks with myelination. Another study performed high-field ex vivo DTI to follow transplantation of immunodeficient *Shi* mice with human neural stem cells (NSCs).<sup>90</sup> The study did not determine AD and RD separately, but an increase of FA was observed in those areas that also showed myelination on histopathology. A recent human phase I study evaluated safety and evidence of myelin formation after transplantation of human CNS stem cells in 4 subjects with an early onset

severe form of PMD.<sup>91</sup> DTI showed an increase of FA and decrease of RD consistent with myelination, in the region of transplantation compared to control white matter regions remote to the transplant sites.

Currently, these techniques all have roles in assessing hypomyelination. MRS shows specific findings in some disorders, but none that is applicable to the entire group of HLDs; it does not allow myelin quantification. MTI is quantitative, and its results are clearly associated with myelin presence, but it is not specific for the binding of water to myelin and therefore will never be precisely quantitative for myelin. DTI is very sensitive to changes in water motion associated with myelination, but the changes in water motion are not specifically caused by myelin; therefore, although very characteristic diffusion changes are caused by myelination, observation of those changes cannot be absolutely interpreted as being the result of myelin, nor can they be used to quantify myelin. Diffusion techniques are likely to improve substantially with technical improvements. MWF, although currently still limited by lack of spatial coverage, time requirements, and frequent technical difficulties that result in artifacts, shows promise for quantitative myelin analysis with technical improvements.

## Emerging Therapies in HLDs

Despite current limitations of MRS, DTI, and MTI in quantifying myelin, these MRI techniques, or a combination thereof, will become particularly important when therapies become available for different HLDs. Because OPCs are defective in HLDs, and the following considerations, cell-based therapies have emerged as candidates for therapeutic research. In preclinical studies, biological properties of OPCs suitable for transplantation include self-renewal and migration.<sup>92</sup> Second, NSCs and OPCs can engraft successfully in mouse models of hypomyelination, conferring functional properties of myelin, such as an enhanced conduction velocity to host axons.<sup>90</sup> A final attribute making HLD a focus of clinical studies is that MRI might comprise a noninvasive method for identifying functional engraftment of myelinating cells in the grossly hypomyelinated background of the host/patient brain.

For these reasons, a 2007 National Multiple Sclerosis Society workshop proposed PMD as a proof of concept disorder for cell-based therapies to restore myelin.<sup>93</sup> These considerations promoted a phase I clinical study of allogeneic NSC transplantation in 4 patients with congenital PMD who were followed clinically and with frequent MRI.<sup>91</sup> These studies showed that the procedure, the immunosuppression, and the transplanted cells themselves were safe 1 year after the transplant. Moreover,

DTI changes in the region of the transplant showed increasing FA and decreasing RD, suggestive of engraftment and consistent with the possibility of myelin formation in those regions. Thus, this study encourages later (phase II/III) testing to prove efficacy of these approaches in HLDs.

However, the outcomes of such studies require expert opinion as to surrogate biomarkers and/or clinical measures that can be employed in the proof of efficacy. By definition, ultrarare disorders have no normal baseline and stereotyped natural history, but rather involve a spectrum of outcomes. To enhance the testing of potential clinical interventions for HLDs, surrogate biomarkers should be adopted as primary outcomes, with careful tracking of clinical outcomes as secondary measures. The following section establishes expert opinion on the current knowledge and research of possible endpoints for clinical trials in HLDs.

### Exploring Surrogate Clinical Endpoints for HLDs

To define clinical endpoints for ultrarare disorders such as HLDs is challenging. Clinical presentation varies from one HLD to another, and complexity is also conferred by individual/developmental changes in the first years of life. For example, classic PMD patients usually have intellectual disability and a complex neurological syndrome consisting of spasticity, ataxia, and an extrapyramidal movement disorder, which is so severe that walking and even sitting without support are not possible. In contrast, patients with the other common HLD, 4H, usually learn to walk without support before their third year of life and have much better cognitive abilities, their main neurological sign being ataxia.<sup>94,95</sup> Even within a given HLD, the spectrum of severity is wide. For PMD, there is clear genotype–phenotype correlation<sup>96,97</sup>; for 4H and other HLDs, this relationship is less obvious. To make things even more complicated, the majority of patients with HLD slowly deteriorate after a period of clinical stability, probably due to axonal degeneration, mirrored in the global atrophy seen in longitudinal imaging (Fig 4).<sup>98</sup>

Observational studies for most HLDs are lacking. Specifically, there is urgent need to study the utility of standardized assessment tools such as the Gross Motor Function Classification System (GMFCS) and dystonia, dyskinesia, and ataxia scales, as well as the applicability of tests of cognitive function in a population with severe motor handicaps. Besides brainstem auditory responses, which are typically absent in PMD, there is no evidence that neurophysiologic or biochemical tools could be used as surrogate outcome markers in HLDs at this point, but

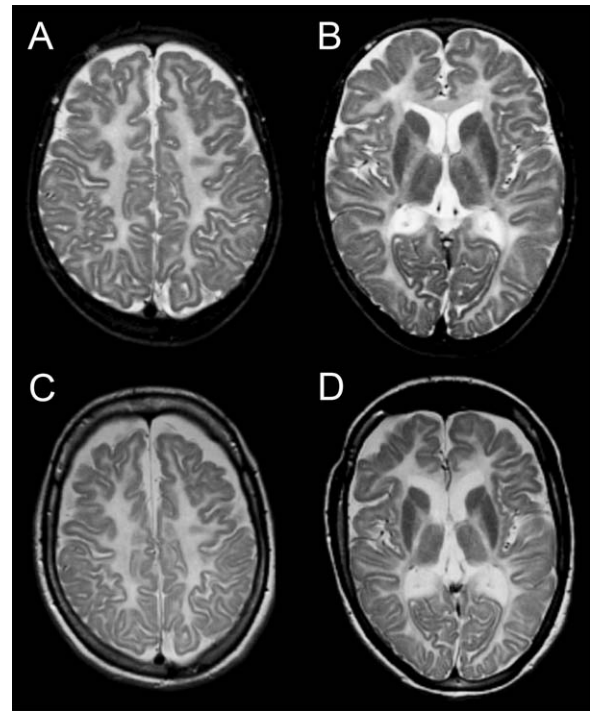


**FIGURE 4:** Global atrophy as shown on longitudinal magnetic resonance imaging. (A, B) Axial T<sub>2</sub>-weighted images of an 8-year-old hypomyelination, hypodontia, and hypogonadotropic hypogonadism patient with a homozygous missense mutation in *POLR3A*. (C, D) Severe global atrophy is visible in the same patient at the age of 19 years, manifested both by an increased volume of cerebrospinal fluid spaces and by a decreased intracranial volume (thicker skull).

this needs further investigations, especially in newly described HLDs.

MRI modalities are currently the most promising surrogate biomarker for clinical trials of HLD, but any improvement seen in MRI surrogates needs correlation with measurable clinical improvement. Of note, MRI modalities that are used as a surrogate biomarker will have to take into consideration any physiologic differences between innate myelination and post-therapeutic remyelination. These may include such considerations as the maturity of myelin wrapping, the hydrophobicity of the myelin membranes, and the size of cytoplasmic channels after myelin wrapping (see Fig 3A). As discussed below, new approaches to quantify myelination may provide the best objective evaluation of effect of a therapeutic trial.

### Exploring Basic and Translational Research to Develop Endpoints for HLDs

#### *New Approaches to Augment Capability of MRI in Myelin Detection in Humans*

The sections above have highlighted scientific opportunities for glial biology and MRI technology to come

together in characterization of myelin disorders. As described above, although MRI techniques do not directly quantify myelin, semiempirical or empirical proton MR models may have promise. For example, several small animal transgenic mouse models exist with hypomyelination and hypermyelination that could be used to “train” MRI methods for greater fidelity. After imaging, the tissue sample or animal would be analyzed for myelin quantity (the “myelin score”) by histology, electron microscopy, and myelin G-ratios (the ratio of axon to myelin circumference).<sup>99</sup> A weighted combination of MR parameters can be selected that best explain the experimentally determined myelin quantities, a process that needs iterative validation. It would be essential to also study animals or samples with inflammatory infiltrates to ensure that a differentiation could be made based on specific parameters (for example, FA, MWF, and MT would be expected to be increased and RD to be decreased with myelination as compared to inflammation). Others have developed myelin-specific gadolinium-complexed MR contrast agents that appear to bind myelin with high specificity and may become clinically useful if they can be modified to cross the blood–brain barrier after intravenous infusion (current compounds require intraventricular infusion).<sup>100</sup> If the compounds bind to myelin in a consistent manner, quantification would potentially be obtainable by relaxometry alone. The goal of these studies would be to refine MRI power to identify myelin quantity *in vivo*.

Several centers have adopted the use of positron emission tomography in clinical studies of multiple sclerosis patients. These studies have used <sup>11</sup>C-labeled N-methyl-4,4'-diaminostilbene<sup>101</sup> to demonstrate accumulation of the compound in myelinating structures in developing animal models, disappearance of the tracer after autoimmune demyelination, and reappearance after remyelination.<sup>102,103</sup> This compound readily crosses the blood–brain barrier and appears to be highly specific for myelinated regions.<sup>101</sup> One disadvantage is exposure of the brain to (relatively low levels of) radiation.

Finally, *in vitro* systems of myelination are helping to define processes that regulate myelin initiation and wrapping.<sup>104</sup> Dual mode imaging incorporating light and/or fluorescent microscopy with simultaneous MRI is envisaged as a way that basic glial biology and MR science might come together to enhance our capabilities for sensitive and specific detection of myelin by MRI.

### **Patient-Specific Models and Potential Therapies for HLDs**

The past decade has seen a revolution in stem cell biology that has resulted in new and promising techniques

for investigation of human disease and patient-specific modeling. Embryonic stem cells (ESCs) are defined by their capacity for self-renewal and totipotency, and mouse and human ESCs can be differentiated into oligodendrocyte-like precursor cells.<sup>100,105,106</sup>

Findings in the past decade have shattered the dogma that differentiation is a one-way process; it is possible to convert fibroblasts back into pluripotent cells.<sup>107,108</sup> Such induced pluripotent stem cells (iPSCs) can be converted into OPC-like progenitors for studies of myelin biology *in vitro*<sup>100</sup> and rescue of the *Shi* mouse *in vivo*.<sup>109</sup> Direct conversion of fibroblasts into OPC-like cells, bypassing the iPSC stage, has recently been demonstrated in rodents.<sup>110,111</sup> Thus, many avenues are available for direct production of OPC-like progenitor cells derived from patient material for *in vitro* and *in vivo* studies to gain new insights into the nature of pathogenic mutations and therapeutic approaches in HLDs.

New technologies for site-specific mutations using TALEN<sup>112</sup> and CRISPR<sup>113,114</sup> technologies make it feasible to create targeted patient-specific mutations to study effects on oligodendrocyte biology, such as engineering patient-specific *PLP1* mutations into ESCs to elucidate their impact on oligodendrocyte maturation, survival, and myelination. Another exciting opportunity may be the reversal of patient-specific mutations through gene correction. Future cell-based therapies for HLDs might proceed from production of iPSCs, gene correction, production of OPCs, and eventual autologous transplantation. However, use of such applications in the brain is likely years away because of safety concerns (eg, potential for oncogenic transformation).

### **Conclusion**

We anticipate that new clinical trials (pharmacological and cell-based therapies) will be forthcoming in the next several decades for HLDs. In ultrarare disorders, clinical trials require biomarker surrogates of efficacy and might be eligible for US Food and Drug Administration Fast Track status. MRI is commonly used in diagnosis of all myelin disorders including HLDs, and is currently the most promising biomarker. We believe it is of utmost importance to prepare for these clinical trials with natural history studies and collection of clinical MRIs. We therefore recommend careful and systematic collection of clinical data via consortiums such as GLIA (Global Leukodystrophy Initiative) and LeukoNet, as well as standardized minimal clinical MRI sequences, including at least DTI, MTI, and combined T<sub>1</sub> and T<sub>2</sub> relaxometry.

Due to the variable clinical presentation of the HLDs, neurological parameters, which can be used as



secondary endpoints, are more difficult to define. Reliable parameters include GMFCS and the appropriate rating scales for spasticity, ataxia, and dystonia. Visually evoked potentials or brainstem auditory evoked potentials might prove to be other objective and easy to use parameters, although they have yet to be validated.

Regarding primary endpoints to be collected in clinical trials, we recommend the following MRI techniques: conventional imaging, MTI (for MTR and MT saturation), DTI (especially for RD and FA), combined  $T_1$  and  $T_2$  relaxometry (for MWF), and proton MRS. Despite the promise of MRI, current individual techniques are not optimized for specific detection of myelin. We propose a multidisciplinary effort to enhance MRI sensitivity using new experimental genetic and humanized animal systems.

Systematic collection of clinical, electrophysiological, and MRI data collection in HLDs in natural history studies will allow us to determine which findings correlate best with MRI characteristics and could therefore represent strong secondary endpoints for future therapeutic trials.

## Acknowledgment

G.B. has received a Research Scholar Junior 1 from the Quebec Health Research Fund and grant support from the Caian Institute in Health Research and Foundation for the Leukodystrophies. S.F.D.-K. has received funding from the Dorothea Schloerzer Program of University of Göttingen, Göttingen, Germany. A.K. received grant support from the LeukoTreat project of the European Commission and Friends of the Children's Clinic Universitäts-Klinikum Eppendorf (UKE).

We thank G. Helman and M. Ulman for editorial assistance, S. Huhn for helpful comments on the manuscript, and the European Leukodystrophies Association for their sponsorship of an international workshop in Leipzig, Germany.

## Authorship

P.J.W.P., A.V., G.B., and N.I.W. and A.J.B. wrote the article and created figures. S.F.D.-K., P.J.W.P., and S.C.L.D. provided expertise regarding MRI modalities. E.B., A.K., W.R., and C.f.-C. provided expertise in myelin biology. A.V., G.B., N.I.W., and W.K. provided expertise regarding the clinical outcomes and classification of hypomyelinating conditions. W.K., D.R., and A.J.B. provided overall revision and coordination of the manuscript. P.J.W.P., A.V., G.B., and N.I.W. share the role of first author for this article. W.K., D.R., and A.J.B. share the role of senior author for this article.

## Potential Conflicts of Interest

G.B.: speaking fees, Actelion Pharmaceuticals, Shire, Genzyme; board membership, Actelion Pharmaceuticals, Shire; NPC registry, Actelion Pharmaceuticals. A.K.: personal fees, BioMarin Pharmaceutical.

## References

- Schiffmann R, Moller JR, Trapp BD, et al. Childhood ataxia with diffuse central nervous system hypomyelination. *Ann Neurol* 1994; 35:331–340.
- Schiffmann R, van der Knaap MS. Invited article: An MRI-based approach to the diagnosis of white matter disorders. *Neurology* 2009;72:750–759.
- Steenweg ME, Vanderver A, Blaser S, et al. Magnetic resonance imaging pattern recognition in hypomyelinating disorders. *Brain* 2010;133:2971–2982.
- Baumann N, Pham-Dinh D. Biology of oligodendrocyte and myelin in the mammalian central nervous system. *Physiol Rev* 2001;81: 871–927.
- Bradl M, Lassmann H. Oligodendrocytes: biology and pathology. *Acta Neuropathol* 2010;119:37–53.
- Funfschilling U, Supplie LM, Mahad D, et al. Glycolytic oligodendrocytes maintain myelin and long-term axonal integrity. *Nature* 2012;485:517–521.
- Morrison BM, Lee Y, Rothstein JD. Oligodendroglia: metabolic supporters of axons. *Trends Cell Biol* 2013;23:644–651.
- Paz Soldán MM, Pirkko I. Biogenesis and significance of central nervous system myelin. *Semin Neurol* 2012;32:9–14.
- Freeman MR, Rowitch DH. Evolving concepts of gliogenesis: a look way back and ahead to the next 25 years. *Neuron* 2013;80: 613–623.
- Baron W, Hoekstra D. On the biogenesis of myelin membranes: sorting, trafficking and cell polarity. *FEBS Lett* 2010;584:1760–1770.
- Webster H. The geometry of peripheral myelin sheaths during their formation and growth in rat sciatic nerves. *J Cell Biol* 1971; 48:348–367.
- Harris JJ, Attwell D. The energetics of CNS white matter. *J Neurosci* 2012;32:356–371.
- Lee Y, Morrison BM, Li Y, et al. Oligodendroglia metabolically support axons and contribute to neurodegeneration. *Nature* 2012;487:443–448.
- Rinholm JE, Hamilton NB, Kessaris N, et al. Regulation of oligodendrocyte development and myelination by glucose and lactate. *J Neurosci* 2011;31:538–548.
- Franklin RJM, French-Constant C. Remyelination in the CNS: from biology to therapy. *Nat Rev Neurosci* 2008;9:839–855.
- Young KM, Psachoulia K, Tripathi RB, et al. Oligodendrocyte dynamics in the healthy adult CNS: evidence for myelin remodeling. *Neuron* 2013;77:873–885.
- Fancy SPJ, Chan JR, Baranzini SE, et al. Myelin regeneration: a recapitulation of development? *Annu Rev Neurosci* 2011;34:21–43.
- Snaidero N, Möbius W, Czopka T, et al. Myelin membrane wrapping of CNS axons by PI(3,4,5)P3-dependent polarized growth at the inner tongue. *Cell* 2014;156:277–290.
- Dhaunchak AS, Colman DR, Nave K-A. Misalignment of PLP/DM20 transmembrane domains determines protein misfolding in Pelizaeus-Merzbacher disease. *J Neurosci* 2011;31:14961–14971.



20. Wolf NI, van der Knaap MS. AGC1 deficiency and cerebral hypomyelination. *N Engl J Med* 2009;361:1997–1998; author reply 1998.
21. Wibom R, Lasorsa FM, Tohonen V, et al. AGC1 deficiency associated with global cerebral hypomyelination. *N Engl J Med* 2009;361:489–495.
22. Magen D, Georgopoulos C, Bross P, et al. Mitochondrial hsp60 chaperonopathy causes an autosomal-recessive neurodegenerative disorder linked to brain hypomyelination and leukodystrophy. *Am J Hum Genet* 2008;83:30–42.
23. Boespflug-Tanguy O, Aubourg P, Dorboz I, et al. Neurodegenerative disorder related to AIMP1/p43 mutation is not a PMLD. *Am J Hum Genet* 2011;88:392–393; author reply 393–395.
24. Feinstein M, Markus B, Noyman I, et al. Pelizaeus-Merzbacher-like disease caused by AIMP1/p43 homozygous mutation. *Am J Hum Genet* 2010;87:820–828.
25. Orthmann-Murphy JL, Enriquez AD, Abrams CK, Scherer SS. Loss-of-function GJA12/connexin47 mutations cause Pelizaeus-Merzbacher-like disease. *Mol Cell Neurosci* 2007;34:629–641.
26. Pingault V, Guiochon-Mantel A, Bondurand N, et al. Peripheral neuropathy with hypomyelination, chronic intestinal pseudo-obstruction and deafness: a developmental "neural crest syndrome" related to a SOX10 mutation. *Ann Neurol* 2000;48:671–676.
27. Tetreault M, Choquet K, Orcesi S, et al. Recessive mutations in POLR3B, encoding the second largest subunit of Pol III, cause a rare hypomyelinating leukodystrophy. *Am J Hum Genet* 2011;89:652–655.
28. Bernard G, Chouery E, Putorti ML, et al. Mutations of POLR3A encoding a catalytic subunit of RNA polymerase Pol III cause a recessive hypomyelinating leukodystrophy. *Am J Hum Genet* 2011;89:415–423.
29. Vanderver A, Tonduti D, Schiffmann R, Schmidt J, Van der Knaap MS. Leukodystrophy overview. 2014. Available at: <http://www.ncbi.nlm.nih.gov/books/NBK184570/>.
30. Takanashi J, Inoue K, Tomita M, et al. Brain N-acetylaspartate is elevated in Pelizaeus-Merzbacher disease with PLP1 duplication. *Neurology* 2002;58:237–241.
31. Takanashi J, Saito S, Aoki I, et al. Increased N-acetylaspartate in mouse model of Pelizaeus-Merzbacher disease. *J Magn Reson Imaging* 2012;35:418–425.
32. Hanefeld FA, Brockmann K, Pouwels PJW, et al. Quantitative proton MRS of Pelizaeus-Merzbacher disease. Evidence of dys- and hypomyelination. *Neurology* 2005;65:701–706.
33. Wilhelm MJ, Ong HH, Wehrli SL, et al. Direct magnetic resonance detection of myelin and prospects for quantitative imaging of myelin density. *Proc Natl Acad Sci U S A* 2012;109:9605–9610.
34. Kreis R, Ernst T, Ross BD. Absolute quantitation of water and metabolites in the human brain. II. Metabolite concentrations. *J Magn Reson* 1993;102:9–15.
35. Barkovich AJ, Kjos BO, Jackson DE Jr, Norman D. Normal maturation of the neonatal and infant brain: MR imaging at 1.5 T. *Radiology* 1988;166:173–180.
36. Kreis R, Ernst T, Ross BD. Development of the human brain: in vivo quantification of metabolite and water content with proton magnetic resonance spectroscopy. *Magn Reson Med* 1993;30:424–437.
37. Kreis R, Hofmann L, Kuhlmann B, et al. Brain metabolite composition during early human brain development as measured by quantitative in vivo <sup>1</sup>H magnetic resonance spectroscopy. *Magn Reson Med* 2002;48:949–958.
38. van der Voorn JP, Pouwels PJW, Hart AAM, et al. Childhood white matter disorders: quantitative MR imaging and spectroscopy. *Radiology* 2006;241:510–517.
39. Takanashi J, Nitta N, Iwasaki N, et al. Neurochemistry in shiverer mouse depicted on MR spectroscopy. *J Magn Reson Imaging* 2014;39:1550–1557.
40. Moffett JR, Ross B, Arun P, et al. N-Acetylaspartate in the CNS: from neurodiagnostics to neurobiology. *Prog Neurobiol* 2007;81:89–131.
41. Gow A, Southwood CM, Lazzarini RA. Disrupted proteolipid protein trafficking results in oligodendrocyte apoptosis in an animal model of Pelizaeus-Merzbacher disease. *J Cell Biol* 1998;140:925–934.
42. Jansen JFA, Shambloot MJ, van Zijl PCM, et al. Stem cell profiling by nuclear magnetic resonance spectroscopy. *Magn Reson Med* 2006;56:666–670.
43. Bloembergen N, Purcell EM, Pound RV. Relaxation effects in nuclear magnetic resonance absorption. *Phys Rev* 1948;73:679–715.
44. Paus T, Collins DL, Evans AC, et al. Maturation of white matter in the human brain: a review of magnetic resonance studies. *Brain Res Bull* 2001;54:255–266.
45. Laule C, Vavasour IM, Leung E, et al. Pathological basis of diffusely abnormal white matter: insights from magnetic resonance imaging and histology. *Mult Scler* 2011;17:144–150.
46. Gelman N, Ewing JR, Gorell JM, et al. Interregional variation of longitudinal relaxation rates in human brain at 3.0T: relation to estimated iron and water contents. *Magn Reson Med* 2001;45:71–79.
47. Hoque R, Ledbetter C, Gonzalez-Toledo E, et al. The role of quantitative neuroimaging indices in the differentiation of ischemia from demyelination: an analytical study with case presentation. In: Alireza M, ed. *International review of neurobiology*. Waltham, MA: Academic Press, 2007:491–519.
48. Menon RS, Rusinko MS, Allen PS. Multiexponential proton relaxation in model cellular systems. *Magn Reson Med* 1991;20:196–213.
49. Mackay A, Whittall K, Adler J, et al. In vivo visualization of myelin water in brain by magnetic resonance. *Magn Reson Med* 1994;31:673–677.
50. Kroeker RM, Henkelman RM. Analysis of biological NMR relaxation data with continuous distributions of relaxation times. *J Magn Reson* 1986;69:218–235.
51. Whittall KP, MacKay AL, Graeb DA, et al. In vivo measurement of T2 distributions and water contents in normal human brain. *Magn Reson Med* 1997;40:34–43.
52. MacKay A, Laule C, Vavasour I, et al. Insights into brain microstructure from the T2 distribution. *Magn Reson Imaging* 2006;24:515–525.
53. Webb S, Munro CA, Midha R, Stanisz GJ. Is multicomponent T2 a good measure of myelin content in peripheral nerve? *Magn Reson Med* 2003;49:638–645.
54. Laule C, Leung E, Li DK, et al. Myelin water imaging in multiple sclerosis: quantitative correlations with histopathology. *Mult Scler* 2006;12:747–753.
55. Laule C, Vavasour IM, Moore GRW, et al. Water content and myelin water fraction in multiple sclerosis. *J Neurol* 2004;251:284–293.
56. Gareau PJ, Rutt BK, Karlik SJ, Mitchell JR. Magnetization transfer and multicomponent T2 relaxation measurements with histopathologic correlation in an experimental model of MS. *J Magn Reson Imaging* 2000;11:586–595.
57. Labadie C, Lee J-H, Rooney WD, et al. Myelin water mapping by spatially regularized longitudinal relaxographic imaging at high magnetic fields. *Magn Reson Med* 2014;71:375–387.
58. Vavasour IM, Laule C, Li DKB, et al. Is the magnetization transfer ratio a marker for myelin in multiple sclerosis? *J Magn Reson Imaging* 2011;33:710–718.

59. Mädler B, Drabycz SA, Kolind SH, et al. Is diffusion anisotropy an accurate monitor of myelination? Correlation of multicomponent T2 relaxation and diffusion tensor anisotropy in human brain. *Magn Reson Imaging* 2008;26:874–888.
60. Oh J, Han ET, Pelletier D, Nelson SJ. Measurement of in vivo multi-component T2 relaxation times for brain tissue using multi-slice T2 prep at 1.5 and 3 T. *Magn Reson Imaging* 2006;24:33–43.
61. Prasloski T, Rauscher A, MacKay AL, et al. Rapid whole cerebrum myelin water imaging using a 3D GRASE sequence. *Neuroimage* 2012;63:533–539.
62. Deoni SCL, Rutt BK, Arun T, et al. Gleaning multicomponent T1 and T2 information from steady-state imaging data. *Magn Reson Med* 2008;60:1372–1387.
63. Lankford CL, Does MD. On the inherent precision of mcDESPOT. *Magn Reson Med* 2013;69:127–136.
64. Deoni SC, Dean DC III, O'Muircheartaigh J. Investigating white matter development in infancy and early childhood using myelin water fraction and relaxation time mapping. *Neuroimage* 2012;63:1038–1053.
65. Kolind S, Matthews L, Johansen-Berg H, et al. Myelin water imaging reflects clinical variability in multiple sclerosis. *Neuroimage* 2012;60:263–270.
66. Kitzler HH, Su J, Zeineh M, et al. Deficient MWF mapping in multiple sclerosis using 3D whole-brain multi-component relaxation MRI. *Neuroimage* 2012;59:2670–2677.
67. Wolff SD, Balaban RS. Magnetization transfer contrast (MTC) and tissue water proton relaxation in vivo. *Magn Reson Med* 1989;11:135–144.
68. Stanisz GJ, Kecojevic A, Bronskill MJ, Henkelman RM. Characterizing white matter with magnetization transfer and T2. *Magn Reson Med* 1999;42:1128–1136.
69. Levesque IR, Pike GB. Characterizing healthy and diseased white matter using quantitative magnetization transfer and multicomponent T2 relaxometry: a unified view via a four-pool model. *Magn Reson Med* 2009;62:1487–1496.
70. Sled JG, Pike GB. Quantitative imaging of magnetization transfer exchange and relaxation properties in vivo using MRI. *Magn Reson Med* 2001;46:923–931.
71. Graham SJ, Henkelman RM. Pulsed magnetization transfer imaging: evaluation of technique. *Radiology* 1999;212:903–910.
72. Odrobina EE, Lam TYJ, Pun T, et al. MR properties of excised neural tissue following experimentally induced demyelination. *NMR Biomed* 2005;18:277–284.
73. Underhill HR, Rostomily RC, Mikheev AM, et al. Fast bound pool fraction imaging of the in vivo rat brain: association with myelin content and validation in the C6 glioma model. *Neuroimage* 2011;54:2052–2065.
74. Mottershead JP, Schmierer K, Clemence M, et al. High field MRI correlates of myelin content and axonal density in multiple sclerosis. *J Neurol* 2003;250:1293–1301.
75. Schmierer K, Tozer DJ, Scaravilli F, et al. Quantitative magnetization transfer imaging in postmortem multiple sclerosis brain. *J Magn Reson Imaging* 2007;26:41–51.
76. Blezer ELA, Bauer J, Brok HPM, et al. Quantitative MRI-pathology correlations of brain white matter lesions developing in a non-human primate model of multiple sclerosis. *NMR Biomed* 2007;20:90–103.
77. Bjarnson TA, Vavasour IM, Chia CLL, MacKay AL. Characterization of the NMR behaviour of white matter in bovine brain. *Magn Reson Med* 2005;54:1072–1081.
78. Stanisz GJ, Webb S, Munro CA, et al. MR properties of excised neural tissue following experimentally induced inflammation. *Magn Reson Med* 2004;51:473–479.
79. Samsonov A, Alexander AL, Mossahebi P, et al. Quantitative MR imaging of two-pool magnetization transfer model parameters in myelin mutant shaking pup. *Neuroimage* 2012;62:1390–1398.
80. Ou X, Sun S-W, Liang H-F, et al. The MT pool size ratio and the DTI radial diffusivity may reflect the myelination in shiverer and control mice. *NMR Biomed* 2009;22:480–487.
81. Ou X, Sun S-W, Liang H-F, et al. Quantitative magnetization transfer measured pool-size ratio reflects optic nerve myelin content in ex vivo mice. *Magn Reson Med* 2009;61:364–371.
82. Dreha-Kulaczewski SF, Brockmann K, Henneke M, et al. Assessment of myelination in hypomyelinating disorders by quantitative MRI. *J Magn Reson Imaging* 2012;36:1329–1338.
83. Basser P, Pierpaoli C. Microstructural and physiological features of tissues elucidated by quantitative-diffusion-tensor MRI. *J Magn Reson B* 1996;111:209–219.
84. Song S-K, Sun S-W, Ramsbottom MJ, et al. Dysmyelination revealed through MRI as increased radial (but unchanged axial) diffusion of water. *Neuroimage* 2002;17:1429.
85. Harsan LA, Poulet P, Guignard B, et al. Brain dysmyelination and recovery assessment by noninvasive in vivo diffusion tensor magnetic resonance imaging. *J Neurosci Res* 2006;83:392–402.
86. Ruest T, Holmes WM, Barrie JA, et al. High-resolution diffusion tensor imaging of fixed brain in a mouse model of Pelizaeus-Merzbacher disease: comparison with quantitative measures of white matter pathology. *NMR Biomed* 2011;24:1369–1379.
87. Wu Y-C, Field AS, Duncan ID, et al. High b-value and diffusion tensor imaging in a canine model of dysmyelination and brain maturation. *Neuroimage* 2011;58:829–837.
88. Pierpaoli C, Basser PJ. Toward a quantitative assessment of diffusion anisotropy. *Magn Reson Med* 1996;36:893–906.
89. Miller E, Widjaja E, Nilsson D, et al. Magnetic resonance imaging of a unique mutation in a family with Pelizaeus-Merzbacher disease. *Am J Med Genet A* 2010;152A:748–752.
90. Uchida N, Chen K, Dohse M, et al. Human neural stem cells induce functional myelination in mice with severe dysmyelination. *Sci Transl Med* 2012;4:155ra136.
91. Gupta N, Henry RG, Strober J, et al. Neural stem cell engraftment and myelination in the human brain. *Sci Transl Med* 2012;4:155ra137.
92. Goldman SA, Nedergaard M, Windrem MS. Glial progenitor cell-based treatment and modeling of neurological disease. *Science* 2012;338:491–495.
93. Duncan I, Goldman S, Macklin W, et al. Stem cell therapy in multiple sclerosis: promise and controversy. *Mult Scler* 2008;14:541–546.
94. Wolf NI, Harting I, Boltshauser E, et al. Leukoencephalopathy with ataxia, hypodontia, and hypomyelination. *Neurology* 2005;64:1461–1464.
95. Bernard G, Thiffault I, Tetreault M, et al. Tremor-ataxia with central hypomyelination (TACH) leukodystrophy maps to chromosome 10q22.3–10q23.31. *Neurogenetics* 2010;11:457–464.
96. Cailloux F, Gauthier-Barichard F, Mimault C, et al. Genotype-phenotype correlation in inherited brain myelination defects due to proteolipid protein gene mutations. Clinical European Network on Brain Dysmyelinating Disease. *Eur J Hum Genet* 2000;8:837–845.
97. Wolf NI, Sistermans EA, Cundall M, et al. Three or more copies of the proteolipid protein gene PLP1 cause severe Pelizaeus-Merzbacher disease. *Brain* 2005;128:743–751.
98. Garbern JY, Yool DA, Moore GJ, et al. Patients lacking the major CNS myelin protein, proteolipid protein 1, develop length-dependent axonal degeneration in the absence of demyelination and inflammation. *Brain* 2002;125:551–561.
99. Rushton WA. A theory of the effects of fibre size in medullated nerve. *J Physiol* 1951;115:101–122.

100. Frullano L, Zhu J, Miller RH, Wang Y. Synthesis and characterization of a novel gadolinium-based contrast agent for magnetic resonance imaging of myelination. *J Med Chem* 2013;56:1629–1640.
101. Wu C, Wang C, Popescu DC, et al. A novel PET marker for in vivo quantification of myelination. *Bioorg Med Chem* 2010;18:8592–8599.
102. de Paula Faria D, de Vries EF, Sijbesma JW, et al. PET imaging of demyelination and remyelination in the cuprizone mouse model for multiple sclerosis: a comparison between [11C]CIC and [11C]MeDAS. *Neuroimage* 2014;87:395–402.
103. Wu C, Zhu J, Baeslack J, et al. Longitudinal positron emission tomography imaging for monitoring myelin repair in the spinal cord. *Ann Neurol* 2013;74:688–698.
104. Lee S, Chong S, Tuck S, et al. A rapid and reproducible assay for modeling myelination by oligodendrocytes using engineered nanofibers. *Nat Protoc* 2013;8:771–782.
105. Brüstle O, Jones KN, Learish RD, et al. Embryonic stem cell-derived glial precursors: a source of myelinating transplants. *Science* 1999;285:754–756.
106. Hu B-Y, Du Z-W, Zhang S-C. Differentiation of human oligodendrocytes from pluripotent stem cells. *Nat Protoc* 2009;4:1614–1622.
107. Takahashi K, Yamanaka S. Induction of pluripotent stem cells from mouse embryonic and adult fibroblast cultures by defined factors. *Cell* 2006;126:663–676.
108. Okita K, Yamanaka S. Induced pluripotent stem cells: opportunities and challenges. *Philos Trans R Soc Lond B Biol Sci* 2011;366:2198–2207.
109. Wang S, Bates J, Li X, et al. Human iPSC-derived oligodendrocyte progenitor cells can myelinate and rescue a mouse model of congenital hypomyelination. *Cell Stem Cell* 2013;12:252–264.
110. Najm FJ, Lager AM, Zaremba A, et al. Transcription factor-mediated reprogramming of fibroblasts to expandable, myelinogenic oligodendrocyte progenitor cells. *Nat Biotechnol* 2013;31:426–433.
111. Yang N, Zuchero JB, Ahlenius H, et al. Generation of oligodendroglial cells by direct lineage conversion. *Nat Biotechnol* 2013;31:434–439.
112. Hockemeyer D, Wang H, Kiani S, et al. Genetic engineering of human pluripotent cells using TALE nucleases. *Nat Biotechnol* 2011;29:731–734.
113. Mali P, Yang L, Esvelt KM, et al. RNA-guided human genome engineering via Cas9. *Science* 2013;339:823–826.
114. Cong L, Ran FA, Cox D, et al. Multiplex genome engineering using CRISPR/Cas systems. *Science* 2013;339:819–823.